

INTENSIVE MONITORING SURVEY OF NEARBY GALAXIES (IMSNG)

MYUNGSHIN IM^{1,2}, CHANGSU CHOI^{1,2}, SUNGYONG HWANG^{1,2}, GU LIM^{1,2}, JOONHO KIM^{1,2}, SOPHIA KIM^{1,2}, GREGORY S. H. PAEK^{1,2}, SANG-YUN LEE^{1,2}, SUNG-CHUL YOON², HYUNJIN JUNG³, HYUN-IL SUNG⁴, YEONG-BEOM JEON⁴, SHUHRAT EHGAMBERDIEV⁵, OTABEK BURHONOV⁵, DAVRON MILZAQULOV⁵, OMON PARMONOV⁵, SANG GAK LEE^{2,6}, WONSEOK KANG⁶, TAEWOO KIM^{6,7}, SUN-GILL KWON⁶, SOOJONG PAK^{1,8}, TAE-GEUN JI^{1,8}, HYE-IN LEE^{1,8}, WOJIN PARK^{1,8}, HOJAE AHN⁹, SEOYEON BYEON⁹, JIMIN HAN⁹, COYNE GIBSON¹⁰, J. CRAIG WHEELER^{10,11}, JOHN KUEHNE¹⁰, CHRIS JOHNS-KRULL¹², JENNIFER MARSHALL¹³, MINHEE HYUN^{1,2}, SEONG-KOOK J. LEE^{1,2}, YONGJUNG KIM^{1,2}, YONGMIN YOON^{1,2}, INSU PAEK^{1,2}, SUHYUN SHIN^{1,2}, YOON CHAN TAAK^{1,2}, JUHYUNG KANG², SEOYEON CHOI¹⁴, MANKEUN JEONG², MOO-KEON JUNG², HWARA KIM¹⁵, JISU KIM⁹, DAYAE LEE¹⁶, BOMI PARK¹, KEUNWOO PARK¹⁷, AND SEONG A O²

¹Center for the Exploration of the Origin of the Universe, Department of Physics and Astronomy, Seoul National University, Gwanak-gu, Seoul 08826, Korea; mim@astro.snu.ac.kr

²Astronomy Program, Department of Physics and Astronomy, Seoul National University, Gwanak-gu, Seoul 151-742, Korea

³Department of Physics, Pohang University of Science and Technology, 77 Cheongam-Ro, Nam-Gu, Pohang, Gyeongbuk 37673, Korea

⁴Korea Astronomy and Space Science Institute, 776 Daedeokdae-ro, Yuseong-gu, Daejeon 34055, Korea

⁵Ulugh Beg Astronomical Institute, Uzbek Academy of Sciences, 33 Astronomical Street, Tashkent 700052, Uzbekistan

⁶National Youth Space Center, Goheung, Jeollanam-do, 59567, Korea

⁷Department of Astronomy and Space Science, Chungbuk National University, Cheongju-City, 28644, Korea

⁸School of Space Research, Kyung Hee University, 1732 Deogyong-daero, Giheung-gu, Yongin-si, Gyeonggi-do 17104, Korea

⁹Department of Astronomy and Space Science, Kyung Hee University, 1732 Deogyong-daero, Giheung-gu, Yongin-si, Gyeonggi-do 17104, Korea

¹⁰McDonald Observatory, The University of Texas at Austin, 3640 Dark Sky Drive, Fort Davis, TX 79734, USA

¹¹Department of Astronomy, The University of Texas at Austin, 2515 Speedway, Austin, TX 78712, USA

¹²Department of Physics & Astronomy, Rice University, 6100 Main St. MS-108, Houston, TX 77005, USA

¹³Mitchell Institute for Fundamental Physics and Astronomy and Department of Physics and Astronomy, Texas A&M University, College Station, TX 77843-4242, USA

¹⁴Phillips Academy, 180 Main St, Andover, MA, 01810, USA

¹⁵Department of Earth Science Education, Seoul National University, Gwanak-gu, Seoul 151-742, Korea

¹⁶Department of Astronomy, Yonsei University, 50 Yonsei-ro, Seodaemun-gu, Seoul 03722, Korea

¹⁷Department of Astronomy and Space Science, Sejong University, 209 Neungdong-ro, Kwangjin-gu, Seoul 05006, Korea

Received November 30, 2018; accepted January 10, 2019

Abstract: Intensive Monitoring Survey of Nearby Galaxies (IMSNG) is a high cadence observation program monitoring nearby galaxies with high probabilities of hosting supernovae (SNe). IMSNG aims to constrain the SN explosion mechanism by inferring sizes of SN progenitor systems through the detection of the shock-heated emission that lasts less than a few days after the SN explosion. To catch the signal, IMSNG utilizes a network of 0.5-m to 1-m class telescopes around the world and monitors the images of 60 nearby galaxies at distances $D < 50$ Mpc to a cadence as short as a few hours. The target galaxies are bright in near-ultraviolet (NUV) with $M_{NUV} < -18.4$ AB mag and have high probabilities of hosting SNe (0.06 SN yr⁻¹ per galaxy). With this strategy, we expect to detect the early light curves of 3.4 SNe per year to a depth of $R \sim 19.5$ mag, enabling us to detect the shock-heated emission from a progenitor star with a radius as small as $0.1 R_{\odot}$. The accumulated data will be also useful for studying faint features around the target galaxies and other science projects. So far, 18 SNe have occurred in our target fields (16 in IMSNG galaxies) over 5 years, confirming our SN rate estimate of 0.06 SN yr⁻¹ per galaxy.

Key words: journals: individual — journals: JKAS

1. INTRODUCTION

Many stars die with dramatic explosions, which we call supernovae (SNe). Understanding the SN explosion has several implications of significant astrophysical importance. For example, type Ia SNe (SNe Ia) have been used as a key distance indicator to understand the expansion of the universe, but the theoretical reason be-

hind the success of SNe Ia as a distance indicator is yet to be clarified. SNe also signify the end of the life of stars and detailed knowledge on SNe completes our understanding on the stellar evolution.

The SN explosion mechanism has been well formulated theoretically. Core-collapse SNe (CC SNe) are neutrino-powered explosions in massive stars and SNe Ia are thermonuclear explosions of white dwarfs (WDs) in close binary systems (Branch & Wheeler

2017). Studies on light curves, spectra, neutrino emission, host galaxies, and remnants of SNe support such an idea. However, direct observational evidence for the proposed SN progenitor star properties is scarce and mostly limited to bright progenitors of SNe II-P (e.g., Smartt et al. 2004; Fraser et al. 2011; Van Dyk et al. 2012a,b, 2013), and efforts are still continuing to gather the observational proof for the SN explosion theoretical framework. Especially, what has been lacking is the evidence whether the progenitor stars have the characteristic sizes as theoretically proposed. For SNe Ia, the progenitor system is thought to be a binary star system with an exploding WD, and the companion star can be either a main sequence or a red giant star (single degenerate system; e.g., Whelan & Iben 1973; Nomoto 1982; Hachisu et al. 1996; Li & van den Heuvel 1997; Langer et al. 2000; Han & Podsiadlowski 2004), or another WD (double degenerate system; e.g., Webbink 1984; Iben & Tutukov 1984; Yoon et al. 2007; Pakmor et al. 2012). The thermonuclear explosion from the merger of a WD and an asymptotic giant branch (AGB) star can also occur (core degenerate system; e.g., Sparks & Stecher 1974; Soker 2015). For CC SNe, a wide range of progenitors are expected, from red supergiants with $R \simeq$ several $100 R_{\odot}$ (Chun et al. 2018) to H/He envelope-stripped progenitors of SNe Ib/Ic with $R \lesssim$ a few R_{\odot} (Yoon et al. 2010). A binary origin of stripped-envelope SNe (i.e., SN I Ib, Ib and Ic) has been suggested, and their progenitor sizes can have a significant diversity from several 100 to $\sim 0.2 R_{\odot}$ (Yoon et al. 2010; Eldridge et al. 2013; Yoon 2015; Yoon et al. 2017; Ouchi & Maeda 2017).

Recently, it has been recognized that the light curve of SN shortly after its explosion contains valuable information about its progenitor system and can be used to set a limit on the progenitor size, R_* (e.g., Kasen 2010; Nakar & Sari 2010; Rabinak & Waxman 2011; Piro & Nakar 2013, 2014; Piro & Morozova 2016; Noebauer et al. 2017). The information is contained in the shock-heated emission that appears shortly after the explosion from the outermost layers of SN ejecta, and, if the progenitor is in a binary system, the companion star that is affected by SN shock. The brightness of the shock-heated emission is proportional to the size of the exploding star (CC SNe) and/or the companion star (SNe Ia). This emission lasts for only a few hours to a few days after the explosion and it is expected to be only $R = -12$ AB mag or fainter for a double degenerate binary progenitor with sizes of 0.01 to $0.1 R_{\odot}$ (Yoon et al. 2007; Pakmor et al. 2012; Tanikawa et al. 2015), but could be brighter for massive stars at $R = -14$ to -16 AB mag for progenitor sizes of 1.0 to $10.0 R_{\odot}$ (see Figure 1).

Despite the difficulties associated with catching the SN shock-heated emission, several groups succeeded in detecting the emission or setting the upper limits on the progenitor stars. For SNe I Ib, Bersten et al. (2012) analyzed the early light curve of SN 2011dh (SN I Ib) and concluded that its progenitor size is $R \simeq 200 R_{\odot}$. The HST images taken two years after the explosion revealed

that the progenitor was indeed a yellow supergiant star with an extended envelope (Van Dyk et al. 2013). For SNe Ia, it has been proven more challenging to catch the shock-heated emission probably due to the fact that the companion star appears to be compact. For example, limits on stellar sizes have been obtained for several SNe Ia from early light curves such as SN 2009ig (Foley et al. 2012), SN 2011fe (Nugent et al. 2011; Bloom et al. 2012), SN 2012cg (Silverman et al. 2012; Shappee et al. 2018), SN 2012ht (Yamanaka et al. 2014), SN 2013dy (Zheng et al. 2013), and a number of low redshift SNe Ia studied by the *Kepler* mission (Olling et al. 2015), all pointing toward small-sized companion stars. However, several results exist that allow a larger companion star. Im et al. (2015b) caught the very early light curve of SN 2015F at 23.9 Mpc using the Lee Sang Gak Telescope (LSGT; Im et al. 2015a). The detection of a possible shock-heated emission suggests that the companion star size is $\lesssim 1 R_{\odot}$. Goobar et al. (2015) studied the shape of the early light curve of SN 2014J, suggesting a large progenitor for this SN Ia. Cao et al. (2015b) claimed a detection of UV flash in the early light curve of another SN Ia, iPTF14atg, again suggesting a very large companion star. Hosseinzadeh et al. (2017) analyzed the early light curve of SN 2017cbv showing that the best fit is obtained when assuming a companion star with a radius of $R = 56 R_{\odot}$. However, they also caution that the blue excess emission could be due to other mechanisms such as circumstellar material interaction. For a review on this subject on both theoretical and observational sides, see Maeda & Terada (2016). Constraints on SNe Ib/Ic are much scarcer than SNe Ia, mostly due to the lack of early light curve data.

To catch the shock-heated emission in the SN early light curve, we are conducting a monitoring survey of nearby galaxies using 1-m class telescopes around the world. The sample is made of galaxies at distances less than 50 Mpc. The galaxies are chosen to be those that have relatively high probabilities of hosting SNe due to its high star formation rate (SFR) and low extinction. The cadence of the observation can be as short as a few hours, but nominally about 1 day. In this paper, we describe this survey, the Intensive Monitoring Survey of Nearby Galaxies (IMSNG). Section 2 describes the target selection criteria, Section 3 describes the observational facilities used by the survey, and Section 4 examines the expected rate of SNe in the IMSNG galaxies. The SNe and other transients that occurred in IMSNG galaxies are given in Section 5, and additional science cases of IMSNG are presented in Section 6. Finally, Section 7 gives the summary and future prospects of the survey.

2. TARGET SELECTION

In general, hundreds of galaxies need to be monitored every night to catch the early light curves of a few SNe per year, since SN rate (SN yr^{-1} per galaxy) is on average of order of 0.01 SN yr^{-1} (e.g., see Graur et al. 2017a). This, however, is not a practical approach since there is a limit on the number of galaxies that can be

covered by a single telescope at a given site.

In order to increase the chance of catching SNe, we examined how host galaxy properties influence the SN rate. It has been known that galaxy properties such as SFR, stellar mass, and specific SFR affect the SN rate (e.g., Botticella et al. 2012; Gao & Pritchett 2013; Graur et al. 2017a,b). CC SNe occur in massive stars that trace star formation activities (e.g., Botticella et al. 2012). Similarly, recent studies suggest that SNe Ia also occur more often in galaxies with higher SFRs (e.g., Smith et al. 2012; Gao & Pritchett 2013; Botticella et al. 2017), with the SN rate being about 10 times higher in star forming galaxies than in passively evolving galaxies (Smith et al. 2012) and the SN rate increasing proportionally with SFR (Smith et al. 2012; Gao & Pritchett 2013). This is so because the distribution of the delay time between the WD detonation and the time of the binary formation is proportional to t^{-1} , preferring SNe Ia with short delay times. Discussions on the delay time distribution and the dependence on SFR can be found in Maoz & Mannucci (2012) and references therein.

Taking into account these factors, we selected our targets to be galaxies based on the following criteria. Note that M_{NUV} is corrected for the Galactic extinction (Bai et al. 2015).

1. $M_{\text{NUV}} < -18.4$ AB mag
2. $D < 50$ Mpc
3. $b > 20$ degree

The first criterion about the NUV magnitude is driven by the fact that SNe occur more frequently in galaxies with high SFR, and NUV is a good proxy for SFR. The NUV magnitude cut roughly corresponds to an SFR of $1 M_{\odot} \text{ yr}^{-1}$. Furthermore, the NUV selection preferentially selects high SFR with little internal extinction. This way, we can expect to detect the shock-heated emission without worrying much about the dust extinction correction that can complicate the light curve analysis. As we shall show later, this NUV magnitude cut provides a galaxy sample whose mean SN rate is about 0.06 SN yr^{-1} – about a factor of six increase above the canonical SN rate.

The second criterion of $D < 50$ Mpc makes it possible to detect the shock-heated emission of SNe with small progenitors. Figure 1 shows the light curve of the shock-heated emission for various sizes of progenitor stars at $D = 50$ Mpc, and a typical SN Ia light curve without shock-heated emission. Two model curve sets are plotted, one for CC SN by Rabinak & Waxman (2011) and another for a companion star in an SN Ia of Kasen (2010). The model parameters are adopted as in Im et al. (2015b). Note that the shock-heated emission from SNe Ia can be anisotropic, and can be about 10 times weaker than the case for the optimal viewing angle which is plotted in Figure 1. With the IMSNG depth of $R = 19.5$ magnitude, Figure 1 demonstrates that we can theoretically expect the detection of the shock-heated emission from a progenitor size of $\sim 1 R_{\odot}$ at $D = 50$ Mpc, under the most optimal condition on the viewing angle and/or the timing of the

observation. At 20 Mpc, we can reach 2 magnitude fainter, and possibly detect the shock-heated emission for a progenitor with $\sim 0.1 R_{\odot}$. Note that merger of a binary WD system may occur in a common envelope that remains during the stellar evolution, and such an event would produce shock-heated emission signal identical to an exploding $\sim 0.1 R_{\odot}$ star (Pakmor et al. 2012; Tanikawa et al. 2015). There are uncertainties in the models too, but considering that the median distance to the IMSNG galaxies is about 30 Mpc, our goal of constraining the progenitor size down to $\sim 1 R_{\odot}$ should be realistic for many of the IMSNG galaxies if not all.

For the shock-heated emission from SNe Ia, there is a degeneracy between the viewing angle and the progenitor size. It is not clear yet how the degeneracy can be broken from the shock-heated emission alone, but we expect to be able to statistically infer the mean size of SNe Ia companion stars once we accumulate a large number of shock-heated emission data (> 10 objects).

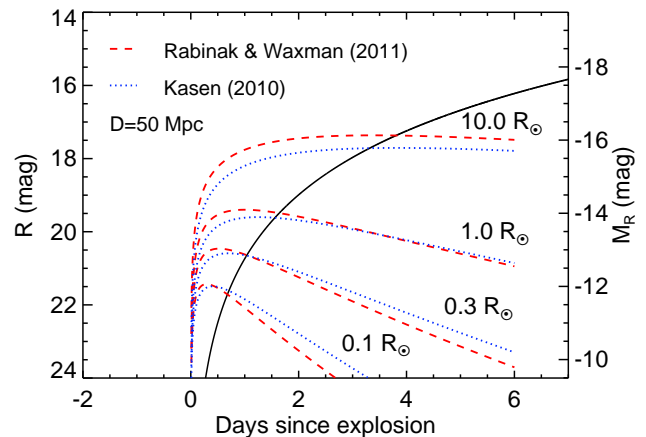


Figure 1. Model predictions of the shock-heated emission light curves at 50 Mpc, overlaid on the best-fit early light curve of SN 2015F (Im et al. 2015b) that is fitted to the data after ~ 1 day after the explosion and shifted to 50 Mpc (the solid black line). The best-fit early light curve of SN 2015F represents a typical SN Ia light curve due to radioactive decay. The dashed lines are for Rabinak & Waxman (2011) for a CC SN, and the dotted lines are for Kasen (2010) due to the shock-heated emission from a companion star in SN Ia. The shock-heated emission from SN Ia is expected to be anisotropic, and can be fainter by 2.5 mag. The case plotted here is for the most optimal viewing angle.

The third criterion is imposed in order to avoid the heavy Galactic extinction and contamination from stars in our Galaxy. However, several galaxies at low Galactic latitude are found to be prolific in SNe or quite bright in M_{NUV} . For this reason, we made two exceptions, and included NGC 6946 and ESO 182-G10 in our sample.

Based on these criteria, we selected galaxies for our monitoring study from the Galaxy Evolution Explorer (GALEX) UV atlas of Gil de Paz et al. (2007) and Bai et al. (2015), where the list of Bai et al. (2015) is a more extended version of Gil de Paz et al. (2007). We started our selection originally from the Gil de Paz et

al. (2007) list and created a list of 46 target galaxies, but now settled on 60 galaxies after expanding the list using the Bai et al. (2015) catalog. Note that there are 22 active galactic nuclei (AGNs) in the 60 IMSNG galaxies¹ – two Seyfert 1.5’s, nine Seyfert 2’s, ten low-ionization nuclear emission line regions (LINERs), and one obscured low luminosity AGN (oLLAGN). So, all of them have either obscured nuclei or low level of AGN, and we can consider their UV luminosities to be dominated by star formation.

The list of the 60 IMSNG galaxies is given in Table 1. Figure 2 shows the M_{NUV} and distance, D , of the IMSNG galaxies.

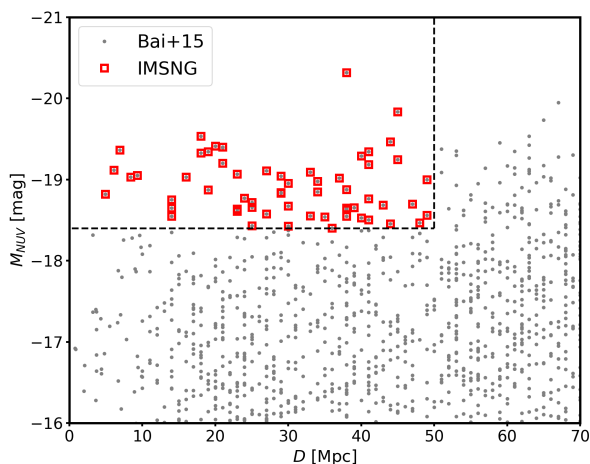


Figure 2. M_{NUV} (AB) versus distance (Mpc) of IMSNG galaxies (red squares), plotted over galaxies from Bai et al. (2015) (gray circles). The area within the black dashed line denotes the region where we selected IMSNG galaxies.

3. FACILITIES

For IMSNG, we use telescopes at multiple locations around the world. This is necessary to cover different time zones and shorten the time cadence to ~ 8 hours. Table 2 lists our current facilities, and Figure 3 shows a map where these facilities are located. Overall, most of our telescopes have field of views of order of 15 to 30 arcmin sizes, except for one wide-field 0.25m telescope with a $2.34^\circ \times 2.34^\circ$ field of view. This 0.25m telescope is a piggyback system on the McDonald Observatory’s 0.8m telescope.

Observations have been carried out nearly every night with LSGT 0.43m, DOAO 1.0m, and the Maidanak 1.5m telescopes (Im et al. 2015a; Ehgamberdiev 2018), but in other locations, the observations have been carried out during time blocks that last about one to two weeks per month. If a galaxy is monitored at Korea, US, and Uzbekistan in one day, this would give roughly an 8 hour cadence. Some equatorial targets can be covered with the telescopes in both hemispheres, and

¹The AGNs are identified through the NASA/IPAC Extragalactic Database at <http://ned.ipac.caltech.edu>.

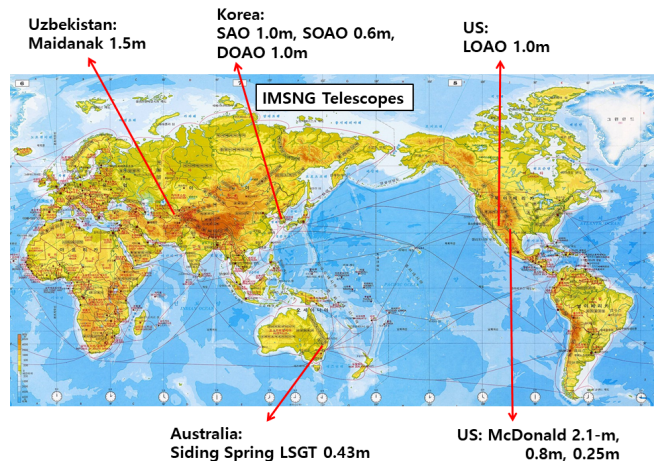


Figure 3. The locations of the telescopes used by IMSNG. The background world map is taken from <http://trip8.co>.

the time cadence can be as short as 2 hours between the observations at Korea and Australia. The exposure times per target vary between facilities from one minute to 5 minutes, and they are set to reach about 19.5 magnitude in R for point-source detection. We mostly use R -band filter for the monitoring observation, although a combination of B and R filters are used at several sites. For some telescopes, r -band filter is used because R -band is not available (LSGT, and the Otto-Struve 2.1m). For the 0.25m telescope, we use V -band since IMSNG galaxies are simultaneously monitored in the other bands with the 0.8m telescope. Multiple filter observations ($BVRI$ or $griz$) are initiated once an SN is identified.

The data taken from each telescope are downloaded to the server at Seoul National University, where they are reduced and analyzed. The data analysis, the transient detection method, and the efficiency of the observation of IMSNG will be presented elsewhere (C. Choi et al. in preparation).

4. SN RATE OF UV-SELECTED GALAXIES

As we described earlier, the key to the success of our program is to select galaxies with high SN rates. We adopted the NUV selection cut for this purpose. Here, we show that SN rates are indeed high for galaxies selected this way. In Figure 4, we show the SN rate per year for galaxies that are selected based on GALEX NUV or far-ultraviolet (FUV) magnitudes. The UV magnitudes are taken from Bai et al. (2015). Galaxies are limited to those at distance less than 50 Mpc for which we can detect faint shock-heated emission. Nearby galaxies have been heavily monitored over the past 10-20 years by professional and amateur astronomers, and we expect that the completeness of SNe discovery rate is very high. To estimate the SN rate, we adopted the period of 2006 to 2016 (11 years), over which the SN discovery completeness should be high thanks to various transient sky surveys. Figure 4 shows that SN rate increases with the UV magnitude in agree-

ment with previous studies that SN rates are higher in galaxies with high SFR (e.g., Botticella et al. 2012; Gao & Pritchett 2013). At the brightest bins in NUV, the rate can go up to 0.2 SN yr^{-1} . Unfortunately, there are only a few galaxies that are very bright in NUV, so we decided to bring down the magnitude limit to $M_{\text{NUV}} = -18.4 \text{ AB mag}$, and at such a limit, we find 0.06 SN yr^{-1} . As we shall show in the next section, our IMSNG results in the recent 5 years agree well with the estimate from the previous 11-year data, suggesting that the completeness of the SNe sampling for the IMSNG galaxies in the 2006 to 2016 period is indeed very high.

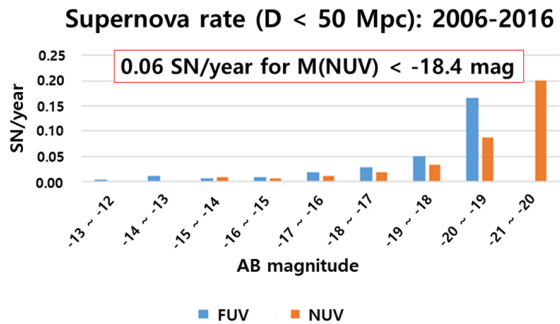


Figure 4. The occurrence of SNe per year per galaxy (SN rate) as a function of FUV (blue) or NUV (red) magnitudes for galaxies within 50 Mpc. The rates were examined over the period of 2006-2016.

5. SNE AND OTHER TRANSIENTS IN IMSNG

As of 2018-12-31 UT, 18 SNe occurred among IMSNG galaxies or in the fields covered by IMSNG over a period of 5 years since the official start of IMSNG in 2014. In addition, other events were also detected such as luminous red novae (LRNe) and eruptions of luminous blue variables (LBVs). These events are summarized in Table 3. In the list, we included a special target, AT2017gfo, the optical counterpart of the gravitational wave source GW170817 (Abbott et al. 2017b; Troja et al. 2017), that was intensively observed using IMSNG facilities, although the host galaxy of AT2017gfo, NGC 4993 (Im et al. 2017b), is not in the IMSNG target list. Excluding one SN that occurred in the field of NGC 895 and another in IC 2163, 16 SNe are divided into 5 SNe Ia, 4 SNe Ib/Ic, and 7 SNe II. The current list of 16 SNe in 60 IMSNG galaxies give an SN rate of 3.2 SN yr^{-1} per 60 galaxies or 0.053 yr^{-1} per galaxy, which is in good agreement with the SN rate of 0.06 SN yr^{-1} that is based on the 11 year period statistics. The SN rates in 2016 and 2018 are low (one per year), but these low rates should be just a statistical fluctuation. The expected $1\text{-}\sigma$ error of the yearly SN rate is $\sqrt{3.4} = 1.8$, and the low rate of one per year is only $1.3\text{-}\sigma$ away from the mean expected rate of 3.4 SN yr^{-1} .

Figure 5 shows an example of an SN event that occurred in one of the IMSNG galaxies. This example shows an IMSNG image of SN 2017gax in NGC 1672 (Im et al. 2017a), before and after its explosion. In

this particular example, our first detection of the SN precedes the date of the image used for the discovery of the event by another group.

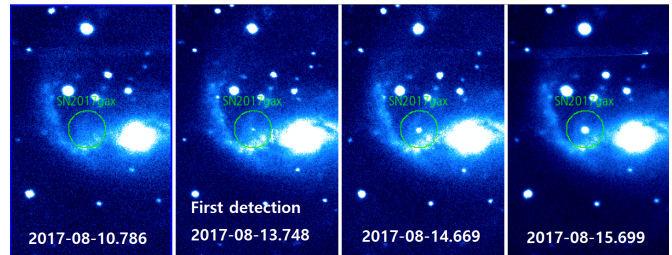


Figure 5. The emergence of SN 2017gax (SN Ib/Ic) in NGC 1672 which is caught by SNUCAM-II on LSGT (Im et al. 2015b; Choi & Im 2017), one of the IMSNG telescopes (Im et al. 2017a). Each image shows a stack of three 180 sec exposure frames in r -band, and the green circle with a radius of $20''$ indicates the location of the SN. This example demonstrates that the high cadence IMSNG observation can catch the early optical light curves of SNe. The UT date of the observation is also indicated in each image.

6. ADDITIONAL SCIENCE CASES

The data gathered from IMSNG are also useful for other projects too. We list several such projects here.

(1) **Other stellar transients:** The transients that can be discovered by IMSNG are not limited to SNe. Two prominent examples are LRNe and LBV outbursts. LRNe are a recently recognized class of transients with their peak luminosities somewhere between novae and SNe at $-14 < M_V < -6 \text{ mag}$ (Kasliwal 2012). LRNe are suggested to be due to the merging of two stars (e.g., Kulkarni et al. 2007), although some think that these are unusually weak SNe IIP (Pastorello et al. 2007). Other physical origins for LRNe have been discussed, such as electron-capture SNe in extreme AGB stars, LBV eruptions, an asteroids crashing to WDs, accretion-induced collapses, and peculiar classical novae (See references in Kasliwal 2012). LBVs are another rare kind of transients arising from evolved massive stars. LBVs undergo giant eruptions, becoming up to a few magnitudes brighter, and when they do so, they are sometimes mistakenly identified as SNe. Hence, they get the name of SN impostor. Both LRNe and LBV outbursts represent unique passages in the stellar evolution. The IMSNG data provide a long-term light curve of the pre-brightening period as well as high cadence light curves after the brightening, which can help us learn about their progenitors and physical origin of the explosive events (e.g., Blagorodnova et al. 2017).

(2) **Merging features and satellite galaxies:** The daily cadence data can be stacked to create deep images of nearby galaxies. The surface brightness (SB) limit of the stacked images can reach $\sim 26.5 \text{ R mag arcsec}^{-2}$ or fainter. At such SB limits, one can identify faint merging features (e.g., see Hong et al. 2015), or new low SB satellite galaxies (e.g., Park et al. 2017).

These features will be useful to understand the merging history of IMSNG galaxies, and the discovery of new satellite galaxies can help understand the problem related to the paucity of dwarf satellite galaxies with respect to the Λ CDM cosmological models. Figure 6 shows an example of a stacked image of 142 frames of one minute images of NGC 895 taken at the Maidanak observatory, corresponding to a total integration time of 2.37 hours, where a faint low SB satellite galaxy candidate and a merging feature around another galaxy are found in the field of NGC 895.

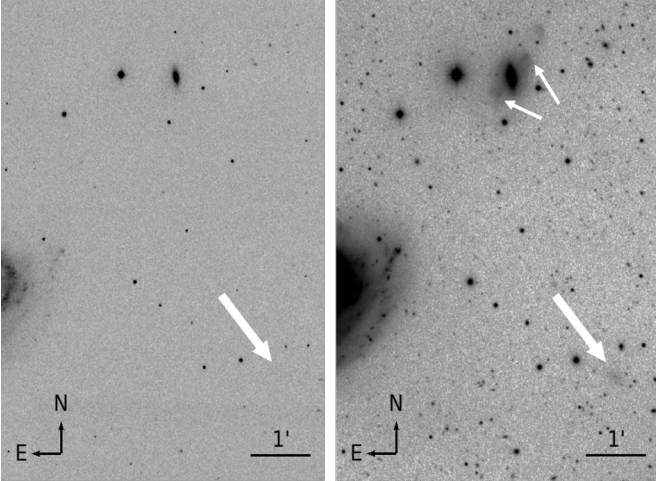


Figure 6. (Left) A single exposure (60 seconds) R -band image near NGC 895 galaxy. A part of NGC 895 is visible on the left. (Right) A stacked R -band image (2.37 hours) of the same field. The data taken from 2013 to 2016 were used. A low SB satellite galaxy candidate is marked as a large, thick arrow. Merging features are visible in the deep image for a galaxy on the top and noted with small arrows.

(3) Gravitational wave source optical counterpart: High cadence monitoring observation offers a unique way to uncover optical counterparts of transients such as gravitational wave (GW) sources. Localization areas of GW sources span tens to hundreds of square degrees, and it is quite common to find several IMSNG galaxies in the localization area. Optical counterparts of GW sources can be searched for IMSNG galaxies and the area surrounding them. One example is SN 2017gax in NGC 1672 which was in the localization area near GW170814, the first GW event with the three detector operation (Abbott et al. 2017a). Eight galaxies were monitored in the localization area at the time of the GW170814 event, and one young SN, SN 2017gax was found in NGC 1672 (Im et al. 2017a). However, our monitoring observation reveals that the SN was present in the image one day before the GW event, ruling out the possibility that SN 2017gax was the GW optical counterpart (Figure 5).

(4) AGNs: Twenty-two of our targets are known AGNs (Seyfert 1.5, Seyfert 2, and LINER galaxies, see Table 1). Their nuclear activities can be traced with our survey at the IMSNG cadence. The monitoring of

the nuclei of IMSNG galaxies could also reveal unexpected AGN activities that can be found only through high cadence monitoring (e.g., Kim et al. 2018). One such example is AT2018ikn which is suggested to be a transient in a Seyfert 2 galaxy, NGC 2992, a possible AGN flare event (Berton et al. 2018).

(5) Variable stars: High cadence observations offer an excellent opportunity to discover new variable stars in the vicinity of IMSNG galaxies. We have searched for new variable stars, and found more than a dozen cases so far (Choi et al. 2018).

(6) Asteroids: Asteroids often appear in the IMSNG data. Their locations can be traced to provide constraints on the orbits of asteroids.

7. SUMMARY & PROSPECTS

In this paper, we gave an overview of IMSNG, which is a monitoring observation project of 60 nearby galaxies at < 50 Mpc with a goal cadence of 8 hours. The main scientific objective of the project is to catch the early light curve of SNe, within one day from the explosion, and constraining the SN progenitor system properties such as the size of the progenitor star. Several such early light curves have been detected among IMSNG galaxies so far (Im et al. 2015b). Nine 1-m class telescopes are currently being used for the monitoring observation. IMSNG galaxies are selected to be galaxies that are bright in NUV ($M_{\text{NUV}} < -18.4$ mag), and we find that the SN rate of the IMSNG galaxies to be about 0.06 SN yr^{-1} using SNe that appeared during the period of 2006-2016, which is six times higher than the SN rate without the UV selection. IMSNG started in 2014, and since then, there have been 16 SNe in the 60 IMSNG galaxies, confirming our SN rate estimate of 0.06 SN yr^{-1} . With the advance of high cadence transient surveys, we expect many SNe to be discovered in their early stages. Yet, a cadence of a few hours is difficult to achieve without employing telescopes at multiple longitudes. In this regard, intensive monitoring observations with small telescopes around the world like IMSNG can cover the niche science where cadence of less than a few hours is desired to the depths of ~ 19.5 mag.

ACKNOWLEDGMENTS

We thank anonymous referees for their useful and constructive suggestions to improve the paper. This research was supported by the Basic Science Research Program through the National Research Foundation of Korea (NRF) funded by the Ministry of Education (NRF-2017R1A6A3A04005158). We thank the staffs at iTelescope.Net, DOAO, LOAO, SOAO, Maidanak & McDonald observatories for their help with the observations and maintenance of the facilities. The research made use of the data taken with LOAO and SOAO operated by the Korea Astronomy and Space Science Institute (KASI), DOAO of National Youth Space Center (NYSC), McDonald Observatory, Maidanak Observatory, and the Siding Spring Observatory.

REFERENCES

- Abbott, B. P., Abbott, R., Abbott, T. D., et al. 2017a, GW170814: A Three-Detector Observation of Gravitational Waves from a Binary Black Hole Coalescence, *PRL*, 119, 141101
- Abbott, B. P., Abbott, R., Abbott, T. D., et al. 2017b, Multi-messenger Observations of a Binary Neutron Star Merger, *ApJL*, 848, 12
- Bai, Y., Liu, J., & Wang, S. 2015, An Updated Ultraviolet Catalog of GALEX Nearby Galaxies, *ApJS*, 220, 6
- Bersten, M. C., Benvenuto, Omar G., Nomoto, K., et al. 2012, The Type IIb Supernova 2011dh from a Supergiant Progenitor, *ApJ*, 757, 31
- Berton, M., Congiu, E., Benetti, S., et al. 2018, ePESSTO Spectroscopic Classification of Optical Transients, *ATel*, 12216
- Blagorodnova, N., Kotak, R., Polshaw, J., et al. 2017, Common Envelope Ejection for a Luminous Red Nova in M101, *ApJ*, 834, 107
- Bloom, J. S., Kasen, D., Shen, K. J., et al. 2012, A Compact Degenerate Primary-star Progenitor of SN 2011fe, *ApJL*, 744, L17
- Botticella, M. T., Cappellaro, E., Greggio, L., et al. 2017, Supernova Rates from The SUDARE VST-Omegacam Search II. Rates in a Galaxy Sample, *A&A*, 598, A50
- Botticella, M. T., Smartt, S. J., Kennicutt, R. C. Jr., Cappellaro, E., Sereno, M., & Lee, J. C. 2012, A Comparison between Star Formation Rate Diagnostics and Rate of Core Collapse Supernovae within 11 Mpc, *A&A*, 537, A132
- Branch, D., & Wheeler, J. C. 2017, *Supernova Explosions: Astronomy and Astrophysics Library* (Berlin: Springer)
- Cao, Y., Kasliwal, M. M., Chen, G., & Arcavi, I. 2015a, iPTF Observation of PSN J14021678+5426205, *ATel*, 7070
- Cao, Y., Kulkarni, S. R., Howell, D., et al. 2015b, A Strong Ultraviolet Pulse from a Newborn Type Ia Supernova, *Nature*, 521, 328
- Choi, C., & Im, M. 2017, Seoul National University Camera II (SNUCAM-II): The New SED Camera for the Lee Sang Gak Telescope (LSGT), *JKAS*, 50, 71
- Choi, N., Park, W.-K., Lee, H.-I., Ji, T.-G., Jeon, Y., Im, M., & Pak, S. 2015, A New Auto-Guiding System for CQUEAN, *JKAS*, 48, 177
- Choi, S., Choi, C., & Im, M. 2018, Photometry of Fifteen New Variable Sources Discovered by IMSNG, *AAVSO*, 46, 1
- Chun, S.-H., Yoon, S.-C., Jung, M.-K., Kim, D. U., & Kim, J. 2018, Evolutionary Models of Red Supergiants: Evidence for a Metallicity-dependent Mixing Length and Implications for Type IIP Supernova Progenitors, *ApJ*, 853, 79
- Ehgamberdiev S. 2018, Modern Astronomy at the Maidanak Observatory in Uzbekistan, *Nature Astronomy*, 2, 349
- Eldridge, J. J., Fraser, M., Smartt, S. J., Maund, J. R., & Crockett, R. M. 2013, The Death of Massive Stars - II. Observational Constraints on The Progenitors of Type Ibc Supernovae, *MNRAS*, 436, 774
- Foley, R. J., Challis, P. J., Filippenko, A. V., et al. 2012, Very Early Ultraviolet and Optical Observations of the Type Ia Supernova 2009ig, *ApJ*, 744, 38
- Fraser, M., Ergon, M., Eldridge, J. J., et al. 2011, SN 2009md: Another Faint Supernova from a Low-mass Progenitor, *MNRAS*, 417, 1417
- Gao, Y., & Pritchett, C. 2013, Correlations between SDSS Type Ia Supernova Rates and Host Galaxy Properties, *AJ*, 145, 83
- Gil de Paz, A., Boissier, S., Madore, B. F., et al. 2007, The GALEX Ultraviolet Atlas of Nearby Galaxies, *ApJS*, 173, 185
- Goobar, A., Kormer, M., Siverd, R., et al. 2015, Constraints on the Origin of the First Light from SN 2014J, *ApJ*, 799, 106
- Goranskij, V. P., Barsukova, E. A., Spiridonova, O. I., et al. 2016, Photometry and Spectroscopy of the Luminous Red Nova PSNJ14021678+5426205 in the Galaxy M101, *Astrophysical Bulletin*, 71, 82
- Graur, O., Bianco, F. B., Huang, S., et al. 2017a, LOSS Revisited. I. Unraveling Correlations between Supernova Rates and Galaxy Properties, as Measured in a Reanalysis of the Lick Observatory Supernova Search, *ApJ*, 837, 120
- Graur, O., Bianco, F. B., Modjaz, M., et al. 2017b, LOSS Revisited. II. The Relative Rates of Different Types of Supernovae Vary between Low- and High-mass Galaxies, *ApJ*, 837, 120
- Hachisu, I., Kato, M., & Nomoto, K. 1996, A New Model for Progenitor Systems of Type Ia Supernovae, *ApJL*, 470, L97
- Han, W., Mack, P., Lee, C.-U., et al. 2005, Development of a 1-m Robotic Telescope System, *PASJ*, 57, 821
- Han, Z., & Podsiadlowski, Ph. 2004, The Single-degenerate Channel for the Progenitors of Type Ia Supernovae, *MNRAS*, 350, 1301
- Hong, J., Im, M., Kim, M., & Ho, L. C. 2015, Correlation between Galaxy Mergers and Luminous Active Galactic Nuclei, *ApJ*, 804, 34
- Hosseinzadeh, G., Sand, D. J., Velenti, S., et al. 1997, Early Blue Excess from the Type Ia Supernova 2017cbv and Implications for Its Progenitor, *ApJL*, 845, L11
- Iben, I. Jr., & Tutukov, A. V., 1984, Supernovae of Type I as End Products of the Evolution of Binaries with Components of Moderate Initial Mass (M not Greater than About 9 Solar Masses), *ApJS*, 54, 335
- Im, M., Choi, C., & Kim, K. 2015a, Lee Sang Gak Telescope (LSGT): A Remotely Operated Robotic Telescope for Education and Research at Seoul National University, *JKAS*, 48, 207
- Im, M., Choi, C., Lee, H. M., et al. 2017a, LIGO/Virgo G297595: LSGT Observation of Nearby Galaxies, *GCN* 21885
- Im, M., Choi, C., Yoon, S.-C., et al. 2015b, The Very Early Light Curve of SN 2015F in NGC 2442: A Possible Detection of Shock-heated Cooling Emission and Constraints on SN Ia Progenitor System, *ApJS*, 221, 22
- Im, M., Ko, J., Cho, Y., Choi, C., Joen, Y., Lee, I., & Ibrahimov, M. 2010, Seoul National University 4K x 4K Camera (SNUCAM) for Maidanak Observatory, *JKAS*, 43, 75
- Im, M., Yoon, Y., Lee, S.-K., et al. 2017b, Distance and Properties of NGC 4993 as the Host Galaxy of the Gravitational-wave Source GW170817, *ApJL*, 849, 16
- Kasen, D. 2010, Seeing the Collision of a Supernova with Its Companion Star, *ApJ*, 708, 1025
- Kasliwal, M. M. 2012, Systematically Bridging the Gap between Novae and Supernovae, *PASA*, 29, 482
- Kim, E., Park, W.-K., Jeong, H., et al. 2011, Auto-Guiding System for CQUEAN (Camera for Quasars in Early Universe), *JKAS*, 44, 115

- Kim, J., Karouzos, M., Im, M., et al. 2018, Intra-Night Optical Variability of Active Galactic Nuclei in the Cosmos Field with the KMTNet, JKAS, 51, 89
- Kim, S., Jeon, Y., Lee, H.-I., et al. 2016, Development of SED Camera for Quasars in Early Universe (SQUEAN), PASP, 128, 5004
- Kulkarni, S., R., Ofek, E. O., Rau, A., et al. 2007, An Unusually Brilliant Transient in the Galaxy M85, Nature, 447, 458
- Langer, N., Deutschmann, A., Wellstein, S., & Hoflich, P. 2000, The Evolution of Main Sequence Star + White Dwarf Binary Systems towards Type Ia Supernovae, A&A, 362, 1046
- Li, X.-D., & van den Heuvel, E. P. J. 1997, Evolution of White Dwarf Binaries: Supersoft X-ray Sources and Progenitors of Type Ia Supernovae, A&A, 322, L9
- Lim, J., Chang, S., Pak, S., Kim, Y., Park, W.-K., & Im, M. 2013, Focal Reducer for CQUEAN (Camera for QUasars in EARly uNiverse), JKAS, 46, 161
- Maeda, K., & Terada, Y. 2016, Progenitors of Type Ia Supernovae, IJMP D, 25, 1630024
- Maoz, D., & Mannucci, F. 2012, Type-Ia Supernova Rates and the Progenitor Problem: A Review, PASA, 29, 447
- Nakar, E., & Sari, R. 2010, Early Supernovae Light Curves Following the Shock Breakout, ApJ, 725, 904
- Noebauer, U. M., Kromer, M., Taubenberger, S., et al. 2017, Early Light Curves for Type Ia Supernova Explosion Models, MNRAS, 472, 2787
- Nomoto, K. 1982, Accreting White Dwarf Models for Type I Supernovae. I - Presupernova Evolution and Triggering Mechanisms, ApJ, 253, 798
- Nugent, P. E., Sullivan, M., Cenko, S. B., et al. 2011, Supernova SN 2011fe from an Exploding Carbon-oxygen White Dwarf Star, Nature, 480, 344
- Olling, R. P., Mushotsky, R., Shaya, E. J., et al. 2015, No Signature of Ejecta Interaction with a Stellar Companion in Three type Ia Supernovae, Nature, 521, 332
- Ouchi, R., & Maeda, K. 2017, Radii and Mass-loss Rates of Type IIb Supernova Progenitors, ApJ, 840, 90
- Pakmor, R., Kromer, M., Taubenberger, S., Sim, S. A., Ropke, F. K., & Hillenbrandt, W. 2012, Normal Type Ia Supernovae from Violent Mergers of White Dwarf Binaries, ApJL, 747, L10
- Park, H. S., Moon, D.-S., Zaritsky, D., et al. 2017, Dwarf Galaxy Discoveries from the KMTNet Supernova Program. I. The NGC 2784 Galaxy Group, ApJ, 848, 19
- Park, W.-K., Pak, S., Im, M., et al. 2012, Camera for Quasars in Early Universe (CQUEAN), PASP, 124, 839
- Pastorello, A., Della Valle, M., Smartt, S. J., et al. 2007, A Very Faint Core-collapse Supernova in M85, Nature, 449, 1
- Piro, A. L., & Morozova, V. S. 2016, Exploring the Potential Diversity of Early Type Ia Supernova Light Curves, ApJ, 826, 96
- Piro, A. L., & Nakar, E. 2013, What Can We Learn from the Rising Light Curves of Radioactively Powered Supernovae?, ApJ, 769, 67
- Piro, A. L., & Nakar, E. 2014, Constraints on Shallow ^{56}Ni from the Early Light Curves of Type Ia Supernovae, ApJ, 784, 85
- Rabinak, I., & Waxman, E. 2011, The Early UV/Optical Emission from Core-collapse Supernovae, ApJ, 728, 63
- Shappee, B. J., Piro, A. L., Stanek, K. Z., et al. 2018, Strong Evidence against a Non-degenerate Companion in SN 2012cg, ApJ, 855, 6
- Silverman, J. M., Ganeshalingam, M., Cenko, S. B., et al. 2012, The Very Young Type Ia Supernova 2012cg: Discovery and Early-time Follow-up Observations, ApJL, 756, L7
- Smartt, S. J., Maund, J. R., Hendry, M. A., et al. 2004, Detection of a Red Supergiant Progenitor Star of a Type II-Plateau Supernova, Sci, 303, 499
- Smith, M., Nichol, R. C., Dilday, B., et al. 2012, The SDSS-II Supernova Survey: Parameterizing the Type Ia Supernova Rate as a Function of Host Galaxy Properties, ApJ, 755, 61
- Soker, N. 2015, The Circumstellar Matter of Supernova 2014J and the Core-degenerate Scenario, MNRAS, 450, 1333
- Sparks, W. M., & Stecher, T. P. 1974, Supernova: The Result of the Death Spiral of a White Dwarf into a Red Giant, ApJ, 188, 149
- Tanikawa, A., Nakasato, N., Sato, Y., Nomoto, K., Maeda, K., & Hachisu, I. 2015, Hydrodynamical Evolution of Merging Carbon-Oxygen White Dwarfs: Their Presupernova Structure and Observational Counterparts, ApJ, 907, 40
- Troja, E., Piro, L., van Eerten, H., et al. 2017, The X-ray Counterpart to the Gravitational-wave Event GW170817, Nature, 551, 71
- Van Dyk, S. D., Cenko, S. B., Poznanski, D., et al. 2012a, The Red Supergiant Progenitor of Supernova 2012aw (PTF12bvh) in Messier 95, ApJ, 756, 131
- Van Dyk, S. D., Davidge, T. J., Elias-Rosa, N., et al. 2012b, Supernova 2008bk and Its Red Supergiant Progenitor, AJ, 143, 19
- Van Dyk, S. D., Zheng, W. K., Clubb, K. I., et al. 2013, The Progenitor of Supernova 2011dh has Vanished, ApJL, 772, L32
- Webbink, R. F. 1984, Double White Dwarfs as Progenitors of R Coronae Borealis Stars and Type I Supernovae, ApJ, 277, 355
- Whelan, J., & Iben, I., Jr. 1973, Binaries and Supernovae of Type I, ApJ, 186, 1007
- Yamanaka, M., Maeda, K., Kawabata, M., et al. 2014, Early-phase Photometry and Spectroscopy of Transitional Type Ia SN 2012ht: Direct Constraint on the Rise Time, ApJL, 782, L35
- Yoon, S.-C. 2015, Evolutionary Models for Type Ib/c Supernova Progenitors, PASA, 32, e015
- Yoon, S.-C., Dessart, L., & Clocchiatti, A. 2017, Type Ib and IIb Supernova Progenitors in Interacting Binary Systems, ApJ, 840, 10
- Yoon, S.-C., Podsiadlowski, P., & Rosswog, S. 2007, Remnant Evolution after a Carbon-oxygen White Dwarf Merger, MNRAS, 380, 933
- Yoon, S.-C., Woosley, S. E., & Langer, N. 2010, Type Ib/c Supernovae in Binary Systems. I. Evolution and Properties of the Progenitor Stars, ApJ, 725, 940
- Zheng, W., Silverman, J. M., Filippenko, A. V., et al. 2013, The Very Young Type Ia Supernova 2013dy: Discovery, and Strong Carbon Absorption in Early-time Spectra, ApJL, 778, L15

Table 1
IMSNG Target Galaxies

Name [AGN type]	RA (J2000)	Dec (J2000)	D _L (Mpc)	NUV (AB)	Past SNe
(1)	(2)	(3)	(4)	(5)	(6)
NGC 289	00:52:42.348	-31:12:20.92	24.0	-18.77	
NGC 337 [LIN]	00:59:50.100	-07:34:41.45	23.0	-18.64	1998dn, 2011dq, 2014cx
NGC 488	01:21:46.836	+05:15:24.48	38.0	-18.88	1976G, 2010eb
NGC 895	02:21:36.468	-05:31:17.00	37.0	-19.02	2003id
NGC 1097 [LIN]	02:46:19.092	-30:16:29.89	14.0	-18.55	1992bd, 1999eu, 2003B
NGC 1309	03:22:06.600	-15:24:00.07	29.0	-19.04	2002fk, 2012Z
NGC 1365 [S1.5]	03:33:36.396	-36:08:25.84	18.0	-19.33	1957C, 1983V, 2001du, 2012fr
UGC 2855	03:48:20.736	+70:07:58.30	14.0	-18.75	2014dg
NGC 1672 [S2]	04:45:42.516	-59:14:50.42	19.0	-19.34	2017gax
NGC 2207/IC 2163 ^a	06:16:22.044	-21:22:21.76	38.0	-20.32	1975A, 1999ec, 2003H, 2010jp, 2013ai, 2018lab
NGC 2336 [S2]	07:27:04.068	+80:10:41.02	29.0	-18.83	1987L
NGC 2442 [LIN]	07:36:23.796	-69:31:50.70	21.0	-19.20	1999ga, 2015F
NGC 2775	09:10:20.100	+07:02:17.23	43.0	-18.69	1993Z
NGC 2776	09:12:14.508	+44:57:17.53	41.0	-19.34	
NGC 2782 [oLLAGN]	09:14:05.064	+40:06:49.57	41.0	-18.76	1994ak
NGC 2993/2992 [S2] ^a	09:45:48.312	-14:22:06.17	34.0	-18.85	2003ao, AT2017ejx
IC 2537	10:03:51.876	-27:34:14.81	36.0	-18.40	2010lm
NGC 3147 [S2]	10:16:53.688	+73:24:02.63	40.0	-19.29	1972H, 1997bq, 2006gi, 2008fv
NGC 3169 [LIN]	10:14:14.892	+03:27:58.86	45.0	-19.25	1984E, 2003cg
NGC 3183	10:21:48.960	+74:10:37.16	49.0	-18.56	
NGC 3244	10:25:28.848	-39:49:39.00	38.0	-18.63	2010ev
NGC 3294	10:36:16.236	+37:19:28.63	30.0	-18.43	1990H, 1992G
NGC 3344	10:43:31.116	+24:55:19.74	20.0	-19.42	2012fh
NGC 3367 [S2]	10:46:35.004	+13:45:02.09	45.0	-19.84	1986A, 1992C, 2003aa, 2007am, 2018kp
NGC 3359	10:46:36.840	+63:13:26.83	23.0	-19.07	1985H
NGC 3445	10:54:35.712	+56:59:23.32	33.0	-18.55	
NGC 3629	11:20:31.776	+26:57:47.84	38.0	-18.55	
NGC 3646	11:21:43.092	+20:10:11.10	44.0	-19.47	1989N, 1999cd
NGC 3938	11:52:49.368	+44:07:14.88	19.0	-18.87	1961L, 1964I, 2005ay, 2017ein
NGC 4030	12:00:23.580	-01:06:00.00	27.0	-19.11	2007aa
NGC 4038 (Arp 244)	12:01:53.004	-18:52:04.76	21.0	-19.40	1921A, 1974E, 2004gt, 2007sr, 2013dk
NGC 4039 (Arp 244)	12:01:53.616	-18:53:11.11	21.0	-19.39	
NGC 4108	12:06:44.316	+67:09:46.12	41.0	-18.50	ASASSN-15lf
NGC 4254 (M 99) [LIN]	12:18:49.572	+14:24:59.08	16.0	-19.03	1967H, 1972Q, 1986I, 2014L
NGC 4303 (M 61) [S2]	12:21:54.936	+04:28:27.05	18.0	-19.54	1926A, 1961I, 1964F, 1999gn, 2006ov, 2008in, 2014dt
NGC 4314 [LIN]	12:22:31.980	+29:53:43.48	44.0	-18.46	1954A
NGC 4321 (M 100) [LIN]	12:22:54.768	+15:49:18.80	14.0	-18.65	2006X
NGC 4500	12:31:22.152	+57:57:52.81	48.0	-18.47	
NGC 4653	12:43:50.916	-00:33:40.54	39.0	-18.66	1999gk, 2009ik
NGC 4814	12:55:21.936	+58:20:38.80	40.0	-18.53	
NGC5194 [S2]/5195 ^a (M51)	13:29:52.692	+47:11:42.54	8.4	-19.03	1945A ^b , 1994I, 2005cs, 2011dh
NGC 5236 (M83)	13:37:00.876	-29:51:56.02	4.9	-18.82	1923A, 1945B, 1950B, 1957D, 1968L, 1983N
NGC 5371 [LIN]	13:55:39.936	+40:27:41.90	33.0	-19.09	1994Y
NGC 5430	14:00:45.720	+59:19:42.24	47.0	-18.70	PTF10acbu (PSN)
NGC 5457 (M101)	14:03:12.600	+54:20:56.62	6.9	-19.36	1909A, 1951H, 1970G, 2011fe
NGC 5584	14:22:23.772	-00:23:15.32	25.0	-18.43	1996aq, 2007af
NGC 5668	14:33:24.300	+04:27:01.19	25.0	-18.72	1952G, 1954B, 2004G
NGC 5850 [LIN]	15:07:07.644	+01:32:40.74	38.0	-18.65	1987B
NGC 5962	15:36:31.680	+16:36:28.15	30.0	-18.68	2016afa, 2017ivu
NGC 6070	16:09:58.680	+00:42:34.31	27.0	-18.58	
NGC 6555	18:07:49.188	+17:36:17.53	35.0	-18.54	
ESO 182-G10 ^c	18:18:30.600	-54:41:39.41	49.0	-19.00	2006ci
NGC 6744 [LIN]	19:09:45.900	-63:51:27.72	9.3	-19.05	2005at
NGC 6814 [S1.5]	19:42:40.608	-10:19:25.32	23.0	-18.61	
NGC 6946 ^{c,d}	20:34:52.572	+60:09:13.57	6.1	-19.12	1980K, 2002hh, 2004et, 2008S, 2017eaw
NGC 6951 [S2]	20:37:14.088	+66:06:20.45	25.0	-18.66	1999el, 2000E, 2015G
NGC 7083	21:35:44.592	-63:54:09.79	34.0	-18.98	1983Y, 2009hm
NGC 7479 [S2]	23:04:56.676	+12:19:22.12	30.0	-18.96	1990U, 2009jf
NGC 7552	23:16:10.776	-42:35:03.41	29.0	-18.84	2017bzc
NGC 7714/7715 ^a	23:36:14.112	+02:09:18.07	41.0	-19.18	1999dn, 2007fo

(1) Galaxy name. The name in the parenthesis is another notable name of the galaxy, and the AGN types in the large parentheses are S (Seyfert), LIN (LINER), and oLLAGN; (2) & (3): Equatorial coordinates in J2000; (4) the luminosity distance; (5) NUV absolute magnitude in AB mag; (6) the past SNe in the galaxy.

^a Galaxies in pair, the primary, NUV-selected galaxy number is given first; ^b In NGC 5195; ^c Low Galactic latitude target; ^d This object had five additional SNe before 1980: 1917A, 1939C, 1948B, 1968D, and 1969P.

Table 2
The current list of telescopes in the IMSNG network

Observatory/ Telescope	Instrument	Imager Field of view	Longitude/ Latitude	Altitude (m)
Maidanak Observatory 1.5m ^a	SNUCAM ^b 4k x 4k	18'3 × 18'3	66:53:47E 38:40:22N	2593
SNU Astronomical Observatory (SAO) 1m ^c	SBIG STX-16803 4k x 4k	21'2 × 21'2	126:57:12E 37:27:25.35N	190
Deokheung Optical Astronomy Observatory (DOAO) 1m	SOPHIA 2k x 2k	13'2 × 13'2	127:26:48E 37:31:35N	81
Sobaeksan Optical Astronomy Observatory (SOAO) 0.6m	PIXIS 2048B 2k x 2k	17'6 × 17'6	128:27:25.3 36:56:03.9N	1340
Lee Sang Gak Telescope (LSGT) 0.43m ^d	SNUCAM-II ^e 1k x 1k	15'7 × 15'7	149:03:52E 31:16:24S	1122
Mt. Lemmon Optical Astronomy Observatory (LOAO) 1m ^f	ARC CCD camera 4k x 4k	28'1 × 28'1	110:47:19.3W 32:26:32.2N	2776
McDonald Observatory (McD) Otto-Struve 2.1m	SQUEAN/CQUEAN ^g 1k x 1k	4'7 × 4'7	104:01:21.4W 30:40:17.4N	2076
McDonald Observatory (McD) 0.8m	CCD camera 2k x 2k	46'2 × 46'2	104:01:19W 30:40:17N	2057
McDonald Observatory (McD) 0.25m	FLI16803 4k x 4k	2.34° × 2.34°	104:01:19W 30:40:17N	2057

Observatories are ordered toward E in longitude from the Prime Meridian.

^a Ehgamberdiev (2018)

^b Im et al. (2010)

^c M. Im et al. (in preparation), <http://sao.snu.ac.kr>

^d Im et al. (2015a)

^e Choi & Im (2017)

^f Han et al. (2005)

^g SQUEAN(Kim et al. 2016; Choi et al. 2015) is the upgraded system of CQUEAN(Park et al. 2012; Lim et al. 2013; Kim et al. 2011)

Table 3
SNe and other transients in IMSNG galaxies (2014-2018)

Name	Type	Host	Notes
2014			
SN 2014L	Ic	M99/NGC 4254	01/26.83, gap in time cov., test obs. period
SN 2014cx	IIP	NGC 337	09/2.275, Maidanak(08/31, 09/03)
ASASSN-14ha	II	NGC 1566	09/10.290, Before LSGT op.
AT2014ej	LBV	NGC 7552	09/24.460
SN 2014dg	Ia	UGC 2855	09/11.725, Before the addition of UGC 2855 in the list
SN 2014dt	Ia	M61/NGC 4303	10/29.838, LOAO/Maidanak out of order
2015			
PSN J14021678+5426205	LRN	M101	2015/01.20.803 ^a
SN 2015F	Ia	NGC 2442	03/09, LSGT daily coverage, Im et al. (2015b)
SN 2015G	Ibn	NGC 6951	03/23.788, altitude too low for LOAO when discovered
ASASSN-15lf	IIn	NGC 4108	06/15.34, Maidanak/LOAO/McD
DES15X2kvt	Ia?	NGC 895	10/02, anonymous Ia in the field?
2016			
SNhunt306	LBV?	NGC 772	02/10.0
AT2016blu/Gaia16ada	LBV	NGC 4559	02/25.723
SN 2016afa	IIP	NGC 5962	02/12.958, Maidanak/LOAO/McD
AT2016jbu	LBV	NGC 2442	12/01.596, LSGT
2017			
SN 2017bzc	Ia	NGC 7552	03/07.219, before sample revision, some LSGT
SN 2017eaw	IIP	NGC 6946	05/14.238, LOAO(5/14), McD(05/05), Maidanak(05/16)
SN 2017ein	Ic	NGC 3938	05/25.969, Maidanak(5/23, 25), DOAO(05/24), McD/LOAO
SN 2017ejx	IIP	NGC 2993	05/30.040, LSGT(05/24,29), LOAO(05/15), DOAO(05/17)
SN 2017gax	Ib/Ic	NGC 1672	08/14.712, LSGT(from 08/13, 14 and on)
AT2017gfo/GW170817	Kilonova	NGC 4993	08/17.98, LSGT, KMTNet
SN 2017ivu	IIP	NGC 5962	12/11.857, altitude too low when discovered
2018			
SN 2018kp	Ia	NGC 3367	01/24.244, daily coverage from McD, DOAO, LOAO
AT2018ikn	AGN flare?	NGC 2992	LSGT
SN 2018lab	II	IC2163	12/29.13, bad weather

The information in Notes include the discovery month and dates in UT, and the primary IMSNG facilities that followed up the event. The dates of observations around the discovery dates are also indicated in the parentheses for events of interest. The object names in bold are the events of interest for which we have an extended dataset before and just after the explosion.

^a After the discovery, the object was found to have $R = 16.36$ mag at 2014-11-10 (UT), which is comparable to the brightness at the discovery time ($V = 17.5$ mag), so the burst could have occurred earlier (Cao et al. 2015a). Also, long-term light monitoring data prior to 2015 suggest that the object was a slow rising source (Goranskij et al. 2016; Blagorodnova et al. 2017).